

# Motion Planning and Collision Avoidance using Navigation Vector Fields

Dimitra Panagou

**Abstract**—This paper presents a novel method on the motion and path planning for unicycle robots in environments with static circular obstacles. The method employs a family of 2-dimensional analytic vector fields, which have singular points of high-order type and whose integral curves exhibit various patterns depending on the value of a parameter  $\lambda$ . More specifically, for a known value of  $\lambda$  the vector field has a unique singular point of dipole type and its integral curves are suitable for steering the unicycle to a goal configuration. Furthermore, for the value of  $\lambda$  that the vector field has a continuum of singular points, the integral curves can be used to define flows around circular obstacles. An almost global feedback motion plan is then constructed by suitably blending attractive and repulsive vector fields in a static obstacle environment. The proposed motion planning and control design is also extended to the multi-agent case, where each agent needs to converge to a desired configuration while avoiding collisions with other agents. The efficacy of the approach is demonstrated via simulation results.

## I. INTRODUCTION

Motion planning, coordination and control for robotic systems still remain an active research topic in many respects. Research within the robotics community has attributed various formulations and methodologies on the motion planning problem, often specialized based on the control objectives and the characteristics of the problems at hand. These methodologies range from Lyapunov-based control methods, to sampling-based planning, to combinatorial planning, see for instance [1]–[3] and the references therein. Furthermore, applications involving multi-robot systems have attracted the interest of the control systems community as well. Emphasis has been given in consensus (also called synchronization, rendezvous or agreement), flocking and formation control problems for multiple agents, see [4] for a very recent survey.

Plausibly, collision avoidance with respect to (w.r.t.) static (stationary) or dynamic (moving) obstacles/agents is a requirement of highest priority in motion planning and coordination problems. One of the most popular ways to formulate and tackle such problems is based on Lyapunov-like scalar functions, see for instance the Avoidance Functions in [5] and the Artificial Potential Fields (APF) in [6]. A very recent survey on addressing multi-agent problems with potential functions' methods is given in [7]. Scalar functions offer the merit of using Lyapunov-based control design and analysis, which not only yield solutions in closed-form, but also offer certain guarantees regarding specified objectives [8].

A drawback of potential functions' methods is the possible appearance of local minima away from the goal point, i.e. of

points in the state space other than the desired equilibrium at which the gradient vector vanishes. This in principle may result in system trajectories that get stuck away from the goal. Certain forms of potential functions may overcome this limitation; namely, navigation functions [9] and harmonic functions [10]. The caveat in the former case is that the Morse property (which guarantees the non-existence of local minima) is rendered after a tuning parameter exceeds a lower bound, which is not a priori known. In the latter case, harmonic functions may be constructed with either discrete or continuous approaches. The computational cost of discrete methods is quite demanding though, yet continuous approaches which employ the analogies of Laplace equation with fluid mechanics may yield closed-form solutions for certain dynamic environments [11]. A recent overview on harmonic potential methods can be found in [12]. Stream functions [13] combine the local-minima-free property of harmonic functions along with hydrodynamic concepts to yield streamlines that are smoother and possibly preferable for second order systems. The method of vortex fields [14] is also relevant to the context, since it uses the anti-gradient of a scalar function to define flows around obstacles.

Attempting now to keep a unifying viewpoint regarding on the use of scalar functions in motion planning and coordination problems, one may argue that a common ground is the resulting *gradient vector field* which, either directly or indirectly, is employed in the control synthesis. More specifically, a single (or multiple) scalar function is defined to encode the environment (e.g. physical obstacles, neighboring agents etc), yielding a gradient vector field which can be used as feedback motion plan. In this sense, it may be plausible as well to pursue to *directly* define vector fields encoding the desired objectives, such as obstacle or collision avoidance. *Yet, to the best of our knowledge, there is not much work addressing such problems with vector field approaches, compared to the extent to which scalar functions have been used.* A notable exception is the recent work by Lindemann and LaValle [15], in which simple smooth vector fields are locally constructed in given convex cell decompositions of polygonal environments, so that their integral curves are by construction collision-free and, in a sequential composition spirit, convergent to a goal point. The method presumes the existence of a high-level discrete motion plan which determines the successive order of the cells from an initial to a final configuration. Recent work employing vector fields for vehicles' navigation is presented also in [16], which is based on the virtual force field method [17], and in [18].

This paper is in part motivated by [15] and presents a novel method on the motion planning and collision avoidance in

The author is with the Coordinated Science Laboratory, College of Engineering, University of Illinois at Urbana-Champaign, Urbana, IL, USA  
dpanagou@illinois.edu

environments with static and/or dynamic obstacles, yielding feedback motion plans for kinematic nonholonomic agents. The method employs a family of two-dimensional analytic vector fields, which have high-order singular points. It is shown that, except for a *known* value of a parameter  $\lambda$ , the vector field has a unique singular point on  $\mathbb{R}^2$ , and moreover that the pattern of the integral curves is suitable for steering a unicycle to a goal configuration. Moreover, for the value of the parameter  $\lambda$  which results in a continuum of singular points, the vector field can be used to define tangential flows around circular obstacles. Consequently, one may define almost global feedback motion plans (i.e. convergent to the goal configuration except for a set of initial conditions of Lebesgue measure zero and collision-free by construction) by blending attractive and repulsive vector fields. This in turn results in simple feedback control laws which force the system to flow along the vector field. The integral curves in the vicinity of the (unavoidable) undesired singularities are similar to those of saddle points, i.e., of unstable equilibria. We furthermore illustrate how the analytic construction of a feedback motion plan and the control design for a single agent can be extended to the collision avoidance and distributed control for multiple nonholonomic agents.

The proposed method does not require to define Lyapunov-like or potential functions encoding the collision avoidance objective and does not suffer from the appearance of sinks (stable nodes) away from goal point. Compared to potential functions that are by construction free of local minima, the approach presented here does not require any parameter tuning to render the desired (almost global) convergence properties; the values of the parameter  $\lambda$  involved in the definition of the vector field are known *a priori*. Compared to methods that rely on vector fields, such as [15], the proposed method *does not* require any cell decomposition of the free space or the existence of a high-level discrete motion plan, and as thus, it is free of any computational complexity issues. Furthermore, it addresses the motion planning and collision avoidance for multiple agents in dynamic environments, and is scalable as the number of agents increases. Note also that the construction presented here is not the same with the one used in earlier work of the author's [19], while it extends the method originally presented in [20] to obstacle environments.

The paper is organized as follows: Section II characterizes the singular points of our vector fields w.r.t. the parameter  $\lambda$ , while Section III presents the construction of the almost global feedback motion plans and the underlying control design. Section IV includes simulations for the static (single agent among obstacles) and the dynamic case (collision avoidance in multi-robot system). Our conclusions and thoughts on future work are summarized in Section V.

## II. ROBOT NAVIGATION VIA VECTOR FIELDS

Consider the motion of a robot with unicycle kinematics in an environment  $\mathcal{W}$  with  $N$  static obstacles. The equations of motion read:

$$\dot{\mathbf{q}} = [\cos \theta \quad \sin \theta \quad 0]^T u + [0 \quad 0 \quad 1]^T \omega, \quad (1)$$

where  $\mathbf{q} = [x \quad y \quad \theta]^T$  is the configuration vector comprising the position  $\mathbf{r} = [x \quad y]^T$  and the orientation  $\theta$  of the robot w.r.t. a global cartesian coordinate frame  $\mathcal{G}$ ,  $u$  is the linear velocity and  $\omega$  is the angular velocity of the robot w.r.t. the body-fixed frame  $\mathcal{B}$ . The robot is modeled as a circular disk of radius  $\rho$ , and each obstacle  $\mathcal{O}_i$  is modeled as a disk of radius  $\rho_{oi}$  centered at  $\mathbf{r}_{oi} = [x_{oi} \quad y_{oi}]^T$ ,  $i \in \{1, \dots, N\}$ . We are interested in constructing a feedback motion plan for steering the robot from (almost) any initial collision-free configuration  $\mathbf{q}_0$  to a final configuration  $\mathbf{q}_f$ .

### A. A family of vector fields for robot navigation

In earlier work of ours' [20] we introduced the class of vector fields  $\mathbf{F} : \mathbb{R}^2 \rightarrow \mathbb{R}^2$  given by:

$$\mathbf{F}(\mathbf{r}) = \lambda(\mathbf{p}^T \mathbf{r})\mathbf{r} - \mathbf{p}(\mathbf{r}^T \mathbf{r}), \quad (2)$$

where  $\lambda \in \mathbb{R}$  is a parameter to be specified later on,  $\mathbf{r} = [x \quad y]^T$  the position vector w.r.t. the global frame  $\mathcal{G}$  and  $\mathbf{p} = [p_x \quad p_y]^T$ ,  $\mathbf{p} \neq \mathbf{0}$ . The analytical form of the vector field components  $F_x, F_y$  is:

$$F_x = (\lambda - 1)p_x x^2 + \lambda p_y x y - p_x y^2, \quad (3a)$$

$$F_y = (\lambda - 1)p_y y^2 + \lambda p_x x y - p_y x^2. \quad (3b)$$

*Theorem 1:* The origin  $\mathbf{r} = \mathbf{0}$  is the unique singular point of the vector field  $\mathbf{F}$  given by (2) if and only if  $\lambda \neq 1$ .

*Proof:* It is straightforward to verify that  $\mathbf{r} = \mathbf{0}$  is a singular point of  $\mathbf{F}$ . Let us write the vector field components (3) of  $\mathbf{F}$  in matrix form as:

$$\begin{bmatrix} F_x \\ F_y \end{bmatrix} = \underbrace{\begin{bmatrix} (\lambda - 1)x^2 - y^2 & \lambda xy \\ \lambda xy & (\lambda - 1)y^2 - x^2 \end{bmatrix}}_{\mathbf{A}(\lambda, \mathbf{r})} \begin{bmatrix} p_x \\ p_y \end{bmatrix}. \quad (4)$$

One has that  $\det(\mathbf{A}(\lambda, \mathbf{r})) = -(\lambda - 1)(x^2 + y^2)^2$ , i.e.  $\mathbf{A}(\lambda, \mathbf{r})$  is nonsingular away from the origin  $x = y = 0$  if and only if  $\lambda \neq 1$ . Then, for  $\lambda \neq 1$  and  $\mathbf{r} \neq \mathbf{0}$ , one has that  $\mathbf{F} = \mathbf{0}$  if and only if  $\mathbf{p} = \mathbf{0}$ . Since  $\mathbf{p} \neq \mathbf{0}$  by definition, we conclude that the vector field  $\mathbf{F}$  given by (2) is nonsingular everywhere but the origin  $\mathbf{r} = \mathbf{0}$ , as long as  $\lambda \neq 1$ . ■

The Jacobian matrix of  $\mathbf{F}$  is singular at  $\mathbf{r} = \mathbf{0}$ , which implies that  $\mathbf{r} = \mathbf{0}$  is a high-order (nonlinear) singularity.

### B. Attractive vector fields

In order to visualize the behavior of the integral curves of  $\mathbf{F}$  around the singular point  $\mathbf{r} = \mathbf{0}$ , we first consider the case for  $\lambda = 2$ . Let us take the vector  $\mathbf{p} = [1 \quad 0]^T$  and write the vector field components as:

$$F_x = x^2 - y^2, \quad (5a)$$

$$F_y = 2xy. \quad (5b)$$

Following [21], the critical point  $\mathbf{r} = \mathbf{0}$  of (5) is a dipole. Dipoles fall into the class of critical points with only elliptic sectors in their neighborhoods; this implies that all integral curves begin at, and end at, the critical point. Furthermore, one may verify out of the phase portrait of the vector field (2) that the integral curves are symmetric w.r.t. the axis of

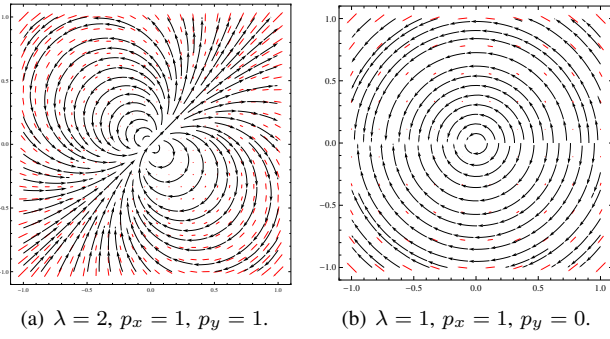


Fig. 1. The vector field  $\mathbf{F}$  for  $\lambda = 2$  and  $\lambda = 1$ .

the vector  $\mathbf{p} \in \mathbb{R}^2$ , see in Fig. 1(a) the integral curves of (2) for  $\lambda = 2$ ,  $\mathbf{p} = [1 \ 1]^T$ . The proofs are available in [22].

In that sense, *any of the integral curves of  $\mathbf{F}$  offers a path to  $\mathbf{r} = \mathbf{0}$ , while the vector  $\mathbf{p}$  dictates the orientation of the integral curves w.r.t. the global frame  $\mathcal{G}$ .* Thus, constructing a feedback motion plan for steering the unicycle to the origin has been based on the following simple idea: Pick  $\mathbf{F}$  out of (2) with  $\lambda = 2$  and  $\mathbf{p} = [p_x \ p_y]^T$  such that the orientation of the vector  $\mathbf{p}$  is zero:  $\varphi_p \triangleq \text{atan2}(p_y, p_x) = 0$ . In this way, the integral curves serve as a reference to steer the orientation trajectories  $\theta(t)$  to zero.

In the sequel, we call the class of vector fields (2) for  $\lambda = 2$  as **attractive** vector fields (or flows) to a configuration  $\mathbf{q} \in \mathbb{R}^2 \times \mathcal{S}$ .

### C. Repulsive vector fields

Let us now investigate the case  $\lambda = 1$ , i.e. the case when the vector field (2) has multiple singular points. The vector field components read:

$$F_x = p_y xy - p_x y^2, \quad (6a)$$

$$F_y = p_x xy - p_y x^2. \quad (6b)$$

To visualize the behavior of the integral curves, let us take  $\mathbf{p} = [1 \ 0]^T$  to get the vector field depicted in Fig. 1(b). One has out of (6) that  $\mathbf{F}$  vanishes on the set  $\mathcal{V} = \{\mathbf{r} \in \mathbb{R}^2 \mid y = 0, x \in \mathbb{R}\}$ . The equation of the integral curves can be computed for  $y \neq 0$  (i.e. away from the singularity set) as:  $\frac{dx}{dy} = \frac{y^2}{-xy} = \frac{y}{-x} \Rightarrow x^2 + y^2 = c^2$  for some  $c \in \mathbb{R}$ , which implies that the integral curves are circular arcs centered at the origin  $\mathbf{r} = \mathbf{0}$ . The phase portrait of  $\mathbf{F}$  furthermore indicates that the integral curves are symmetric w.r.t. the axis  $y = 0$ , i.e., w.r.t. the singularity set  $\mathcal{V}$ , and also that the singularity set is dictated by the orientation  $\varphi_p = 0$  of the vector  $\mathbf{p}$ . The proofs on the symmetric properties of the vector fields are available online in [22].

What is of main interest in this case is that the signum of  $x$  dictates whether the integral curves escape the singularity set  $\mathcal{V}$  (see the half-plane  $x > 0$ ) or converge to the singularity set  $\mathcal{V}$  (see the half-plane  $x < 0$ ). We say that the singular point  $\mathbf{r} = \mathbf{0}$  of the vector field (6) is of center type; this means that *no integral curve reaches the singular point*.<sup>1</sup>

<sup>1</sup>This is slightly inconsistent with standard notation, since the critical point  $\mathbf{r} = \mathbf{0}$  is not isolated.

One may also note that the departing behavior of the integral curves away from the singularity set  $\mathcal{V}$  resembles the pattern of a fluid flow around a cylinder. This actually motivates us to employ (6) in order to define tangential vector fields locally around circular obstacles.

In the sequel we call the class of vector fields (2) for  $\lambda = 1$  as **repulsive** vector fields (or flows) around a point  $\mathbf{r} \in \mathbb{R}^2$ .

### III. ALMOST GLOBAL FEEDBACK MOTION PLANS

Given the class of attractive and repulsive vector fields, the idea on defining an almost global feedback motion plan  $\mathbf{F}^*$  on the collision-free space  $\mathcal{F}$  is now simple: we pursue to combine an attractive-to-the-goal vector field  $\mathbf{F}_g$  with (local) repulsive vector fields  $\mathbf{F}_{oi}$  around each obstacle  $\mathcal{O}_i$ , so that the integral curves of  $\mathbf{F}^*$ : 1) converge to the goal  $\mathbf{q}_g$ , and 2) point into the interior of  $\mathcal{F}$  on the boundaries of the obstacles  $\mathcal{O}_i$ . The vector field  $\mathbf{F}^*$  can then serve as a safe feedback motion plan in  $\mathcal{W}$ . Blending the vector fields  $\mathbf{F}_g$ ,  $\mathbf{F}_{oi}$  should be done in a careful way, so that  $\mathbf{F}^*$  does not have any undesired singularities on  $\mathcal{F}$ .

*Remark 1:* In the sequel, when we refer to  $\mathbf{F}_g$ ,  $\mathbf{F}_{oi}$  we assume the corresponding *normalized unit vector fields*, i.e., the vector fields  $\frac{\mathbf{F}_g}{\|\mathbf{F}_g\|}$ ,  $\frac{\mathbf{F}_{oi}}{\|\mathbf{F}_{oi}\|}$ , with  $\|\cdot\|$  denoting the standard Euclidean norm.

We assume without loss of generality that the goal configuration is the origin,  $\mathbf{q}_g = \mathbf{0}$ . The attractive-to-the-goal vector field  $\mathbf{F}_g$  may then be taken out of (2) for  $\lambda = 2$ ,  $\mathbf{p}_g = [1 \ 0]^T$ , so that  $\varphi_p = 0$ , yielding the vector field (5).

Let us now define a repulsive vector field  $\mathbf{F}_{oi}$  in a region  $\mathcal{Z}_i$  around an obstacle  $\mathcal{O}_i$ . The region  $\mathcal{Z}_i$  is defined as a circular disk centered at  $\mathbf{r}_{oi}$  with radius  $\rho_{\mathcal{Z}_i} = \rho_{oi} + \rho_\varepsilon + \rho$ , where  $\rho_\varepsilon \geq 0$ ; this parameter is the minimum distance that the robot will keep w.r.t. the boundary of the obstacle  $\mathcal{O}_i$ , see Fig. 2. A repulsive vector field w.r.t. the point  $\mathbf{r}_{oi}$  can then be defined out of (6) for  $\lambda = 1$  as:

$$F_{oxi} = p_{yi}(x - x_{oi})(y - y_{oi}) - p_{xi}(y - y_{oi})^2, \quad (7a)$$

$$F_{oyi} = p_{xi}(x - x_{oi})(y - y_{oi}) - p_{yi}(x - x_{oi})^2, \quad (7b)$$

where  $p_{xi} \triangleq \cos \phi_i$ ,  $p_{yi} \triangleq \sin \phi_i$ ,  $\phi_i \triangleq \text{atan2}(-y_{oi}, -x_{oi}) + \pi$ . Note that the vector  $\mathbf{p}_i$  is picked to lie on the line connecting the center  $(x_{oi}, y_{oi})$  of the obstacle with the goal point  $(0, 0)$ . By doing so, we impose the set of singular points of (7) to lie on this line. Furthermore, the integral curves of (7) depart from the singularity set in the region  $\mathcal{A}_i = \{\mathbf{r} \in \mathbb{R}^2 \mid \mathbf{p}_i^T(\mathbf{r} - \mathbf{r}_{oi}) \geq 0\}$  (see also the red vectors around the set  $\mathcal{V}_i$  in Fig. 2), and converge to the singularity set in the region  $\mathcal{B}_i = \{\mathbf{r} \in \mathbb{R}^2 \mid \mathbf{p}_i^T(\mathbf{r} - \mathbf{r}_{oi}) < 0\}$  (the corresponding vectors have *not* been drawn in Fig. 2).

The pattern of the (departing) integral curves in the neighborhood of the singularity set  $\mathcal{V}_i$  in region  $\mathcal{A}_i$  is desirable, since it renders safe, tangential reference paths around the obstacle  $\mathcal{O}_i$ . However, the pattern of the integral curves around the singularity set in region  $\mathcal{B}_i$  is undesirable, since it may trap the system trajectories  $\mathbf{r}(t)$  away from the origin. This limitation is overcome by defining a vector field (2) for  $\lambda = 0$  and  $\mathbf{p}_i$  as before, in region  $\mathcal{B}_i$ ; the resulting integral

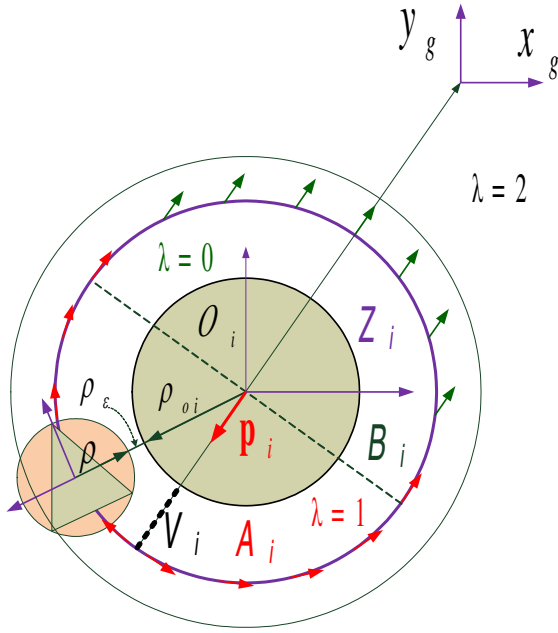


Fig. 2. Defining a repulsive vector field  $\mathbf{F}_{oi}$  around the obstacle  $\mathcal{O}_i$ . Take the vector field (2) with  $\lambda = 1$  in region  $\mathcal{A}_i$  and with  $\lambda = 0$  in region  $\mathcal{B}_i$ .

curves for  $\lambda = 0$  are co-linear with, while pointing to the opposite direction w.r.t.  $\mathbf{p}_i$ , see Fig. 2.

In summary, the vector field  $\mathbf{F}_{oi}$  around an obstacle  $\mathcal{O}_i$  is picked out of the family of vector fields (2) as:

$$\mathbf{F}_{oi} = \begin{cases} \mathbf{F}|_{\lambda=1}(\delta \mathbf{r}_i), & \text{for } \mathbf{p}_i^T(\delta \mathbf{r}_i) \geq 0; \\ \mathbf{F}|_{\lambda=0}(\delta \mathbf{r}_i), & \text{for } \mathbf{p}_i^T(\delta \mathbf{r}_i) < 0, \end{cases} \quad (8)$$

where  $\mathbf{p}_i = [\cos \phi_i \quad \sin \phi_i]^T$ ,  $\phi_i \triangleq \text{atan2}(-y_{oi}, -x_{oi}) + \pi$ ,  $\delta \mathbf{r}_i \triangleq \mathbf{r} - \mathbf{r}_{oi}$ . Note that the transition of the integral curves between regions  $\mathcal{A}_i$ ,  $\mathcal{B}_i$  is smooth, since the vectors at the points  $\mathbf{p}_i^T(\mathbf{r} - \mathbf{r}_{oi}) = 0$  coincide.

The effect of the repulsive vector field  $\mathbf{F}_{oi}$  (8) should be restricted into the region  $\mathcal{Z}_i$ , while away from  $\mathcal{Z}_i$  the effect of the attractive vector field  $\mathbf{F}_g$  should drive the robot to the goal. To encode this requirement, we first define the obstacle function  $\beta_i(\cdot) : \mathbb{R}^2 \rightarrow \mathbb{R}$  as:

$$\beta_i = \rho_{oi}^2 - (x - x_{oi})^2 - (y - y_{oi})^2, \quad (9)$$

which is positive in the interior of the obstacle  $\mathcal{O}_i$ , zero on the boundary of the obstacle, and negative everywhere else. The value of the constraint function  $\beta_i$  on the boundary of  $\mathcal{Z}_i$  is:  $\beta_{iZ} = -2\rho_{oi}(\rho + \rho_\epsilon) - (\rho + \rho_\epsilon)^2$ . Thus, one equivalently has:  $\mathcal{Z}_i = \{\mathbf{r} \in \mathbb{R}^2 \mid \beta_{iZ} \leq \beta_i(\mathbf{r}) \leq 0\}$ .

Consequently, the repulsive vector field  $\mathbf{F}_{oi}$  should be defined for  $\beta_i(\mathbf{r}) \geq \beta_{iZ}$ , while the effect of the attractive vector field  $\mathbf{F}_g$  should be restricted in the region exterior to  $\mathcal{Z}_i$ , i.e. for  $\beta_i(\mathbf{r}) < \beta_{iZ}$ . To encode this, we define the smooth bump function  $\sigma_i(\cdot) : \mathbb{R}^2 \rightarrow [0, 1]$  as:

$$\sigma_i = \begin{cases} 1, & \text{for } \beta_i(\mathbf{r}) \leq \beta_{iF}; \\ a\beta_i^3 + b\beta_i^2 + c\beta_i + d, & \text{for } \beta_{iF} < \beta_i(\mathbf{r}) < \beta_{iZ}; \\ 0, & \text{for } \beta_{iZ} \leq \beta_i(\mathbf{r}); \end{cases} \quad (10)$$

where  $\beta_{iZ}$  is the value of the constraint (9) on the boundary of  $\mathcal{Z}_i$ ,  $\beta_{iF}$  is the value of the constraint (9) at some distance  $\rho_{Fi} > \rho_{Zi}$ , and the coefficients  $a$ ,  $b$ ,  $c$  and  $d$  have been computed as:  $a = \frac{2}{(\beta_{iZ} - \beta_{iF})^3}$ ,  $b = -\frac{3(\beta_{iZ} + \beta_{iF})}{(\beta_{iZ} - \beta_{iF})^3}$ ,  $c = \frac{6\beta_{iZ}\beta_{iF}}{(\beta_{iZ} - \beta_{iF})^3}$ ,  $d = \frac{\beta_{iZ}^2(\beta_{iZ} - 3\beta_{iF})}{(\beta_{iZ} - \beta_{iF})^3}$ , so that (10) is a  $\mathcal{C}^2$  function. Having this at hand, and inspired by [15], one may now define the vector field:

$$\mathbf{F} = \sigma_i \mathbf{F}_g + (1 - \sigma_i) \mathbf{F}_{oi}, \quad (11)$$

which is: (i) attractive to the goal  $\mathbf{q}_g$  sufficiently away from  $\mathcal{O}_i$  via the effect of  $\mathbf{F}_g$  (i.e. for  $\beta_i \leq \beta_{Fi}$ , where one has  $\sigma_i = 1$ ), and (ii) repulsive w.r.t. the obstacle  $\mathcal{O}_i$  in the region  $\mathcal{Z}_i$  via the effect of  $\mathbf{F}_{oi}$  (i.e. for  $\beta_{Zi} \leq \beta_i$ , where one has  $\sigma_i = 0$ ). To check whether singularities occur in the region where  $\beta_{Zi} < \beta_i < \beta_{Fi}$ , let us consider the blending of  $\mathbf{F}_g$  with  $\mathbf{F}_{oi}$  in the exterior of the region  $\mathcal{B}_i$ . The norm of  $\mathbf{F}$  reads:  $\|\mathbf{F}\| = \sqrt{\sigma_i^2 \|\mathbf{F}_g\|^2 + (1 - \sigma_i)^2 \|\mathbf{F}_{oi}\|^2 + 2\sigma_i(1 - \sigma_i)[\mathbf{F}_g \cdot \mathbf{F}_{oi}]}$ . Given that we consider the normalized unit vector fields this further reads:  $\|\mathbf{F}\| = \sqrt{-2\sigma_i(1 - \sigma_i) + 1 + 2\sigma_i(1 - \sigma_i)\cos \alpha}$ , where  $\alpha$  the angle between the vectors  $\mathbf{F}_g$ ,  $\mathbf{F}_{oi}$  at some point  $(x, y)$ . After some more algebra, we have that the norm  $\|\mathbf{F}\|$  vanishes at the points  $\mathbf{r} \in \mathbb{R}^2$  where  $\sigma_i$  is the solution of the quadratic equation:  $2(\cos \alpha - 1)\sigma_i^2 - 2(\cos \alpha - 1)\sigma_i - 1 = 0$ ; yet, this equation does not have any real solutions. The same procedure can be done for the blending of  $\mathbf{F}_g$ ,  $\mathbf{F}_{oi}$  in the exterior of the region  $\mathcal{A}_i$ , with the caveat that here the vector field  $\mathbf{F}_{oi}$  has by construction a singularity set. Then, away from the singularities of  $\mathbf{F}_{oi}$  one eventually gets the same result as above, while for the points where  $\mathbf{F}_{oi} = \mathbf{0}$  one eventually has:  $\|\mathbf{F}\| = \sigma_i \neq 0$ . Consequently, the blending of  $\mathbf{F}_g$ ,  $\mathbf{F}_{oi}$  does not result in any singularities in the blending region  $\beta_{Zi} < \beta_i < \beta_{Fi}$ .

It is now easy to extend the proposed vector field design in the case of  $N$  static obstacles and define an almost global feedback motion plan in  $\mathcal{F}$  as:

$$\mathbf{F}^* = \prod_{i=1}^N \sigma_i \mathbf{F}_g + \sum_{i=1}^N (1 - \sigma_i) \mathbf{F}_{oi}, \quad (12)$$

where  $\mathbf{F}_g$  is the attractive vector field (5),  $\mathbf{F}_{oi}$  is the repulsive vector field (8) around an obstacle  $\mathcal{O}_i$ ,  $i \in \{1, \dots, N\}$ , and  $\sigma_i$  is the bump function (10) defined in terms of the obstacle function  $\beta_i$  (9). The first term in (12) cancels the effect of the attractive vector field  $\mathbf{F}_g$  everywhere that at least one of the bump functions  $\sigma_i = 0$ , i.e. in the corresponding region  $\mathcal{Z}_i$  around the obstacle  $\mathcal{O}_i$ , while at the same time the second term shapes the corresponding vector field  $\mathbf{F}_{oi}$  in  $\mathcal{Z}_i$ . In other words, the attractive vector field  $\mathbf{F}_g$  is activated through (12) only when  $\beta_i < \beta_{Zi} \forall i \in \{1, \dots, N\}$ , i.e. outside the regions  $\mathcal{Z}_i$ .

For  $\mathbf{F}^*$  being an everywhere collision-free feedback motion plan, the clearance among obstacles should be sufficiently large so that the repulsive flows do not overlap. This means that the distance  $d_{ij} = \|\mathbf{r}_{oi} - \mathbf{r}_{oj}\|$  among every pair of obstacles  $\mathcal{O}_i$ ,  $\mathcal{O}_j$  should be at least  $\rho_{Zi} + \rho_{Zj}$ ,

or equivalently, that the minimum distance between the boundaries of two obstacles should be at least  $2(\rho + \rho_\varepsilon)$ . Note that this clearance is not conservative or restrictive in practice, since the parameter  $\rho_\varepsilon$  can be chosen arbitrarily close to zero, or even equal to zero, assuming that the robot is allowed to touch the obstacle. In this case the minimum clearance is equal to  $2\rho$ , i.e., to the diameter of the robot.

The sets of singular points  $\mathcal{V}_i, i \in \{1, \dots, N\}$  are located in the regions  $\mathcal{A}_i$  around the obstacles  $\mathcal{O}_i$ , as shown in Fig. 2. Take the singular point in  $\mathcal{V}_i$  which lies on the boundary of  $\mathcal{Z}_i$ , and let us consider the pattern of the integral curves around this point. The integral curves around  $\mathcal{V}_i$  are departing the set, except for one integral curve that may converge to  $\mathcal{V}_i$ ; it is easy to see that this may happen in the case when the goal orientation  $\theta_g$  is co-linear with the line the singularity set  $\mathcal{V}_i$  lies on. This in turn happens only if the obstacle is positioned such that the direction of the vector  $\mathbf{p}_i$  coincides with the direction of the vector  $\mathbf{p}_g$ . In this case, the set of initial conditions that converge to the singularity sets of  $\mathbf{F}^*$  is of Lebesgue measure zero. In any other case, then: 1) if  $\rho_\varepsilon \neq 0$ , then the singular points are confined in the region  $\mathcal{Z}_i$  on a line segment of length  $\rho_\varepsilon$ , and correspond to the initial conditions from which solutions are not defined, 2) if  $\rho_\varepsilon = 0$ , then the (unique) singular point lies on the boundary of  $\mathcal{Z}_i$  and is reached by no integral curve.

With this at hand, the control design for the unicycle (1) is now straightforward. We use the control law:

$$u = k_u \tanh(x^2 + y^2), \quad (13a)$$

$$\omega = -k_\omega(\theta - \varphi) + \dot{\varphi}, \quad (13b)$$

where  $\varphi \triangleq \arctan(F_y^*, F_x^*)$  is the orientation of the vector field  $\mathbf{F}^*$  at a point  $(x, y)$ , and  $k_\omega, k_u > 0$ , so that the orientation  $\theta$  of the unicycle is globally exponentially stable to the orientation  $\varphi$ . Then, the vehicle flows along the integral curves of  $\mathbf{F}^*$ , until converging to the goal point  $\mathbf{q}_g = \mathbf{0}$ .

#### IV. SIMULATION RESULTS

The efficacy of the proposed motion planning and control design in environments with static obstacles, as well as for the collision avoidance in multi-agent systems, is demonstrated via simulation results.

The vector field  $\mathbf{F}^*$  in an environment populated with  $N = 10$  static obstacles is depicted in Fig. 3 with the goal point being the origin,  $\mathbf{q}_g = \mathbf{0}$ . The resulting path under the control law (13), with the control gains picked equal to  $k_u = 0.1, k_\omega = 1$ , is depicted in red color. Note that the pattern of the integral curves of  $\mathbf{F}_{oi}$  in the regions  $\mathcal{A}_i$  around obstacles forces the robot to approach close to the obstacles and then perform a sharp maneuver in order to follow the tangential direction and avoid collision. Although this in practice is plausible for unicycle-type vehicles (e.g. differentially driven mobile robots), it might not be desirable for input-constrained vehicles, such as car-like vehicles and aircrafts. Thus, our current work focuses in encoding curvature constraints via the family of vector fields (2).

Following the same spirit the proposed control design (13) can be employed for avoiding collisions in the multi-agent

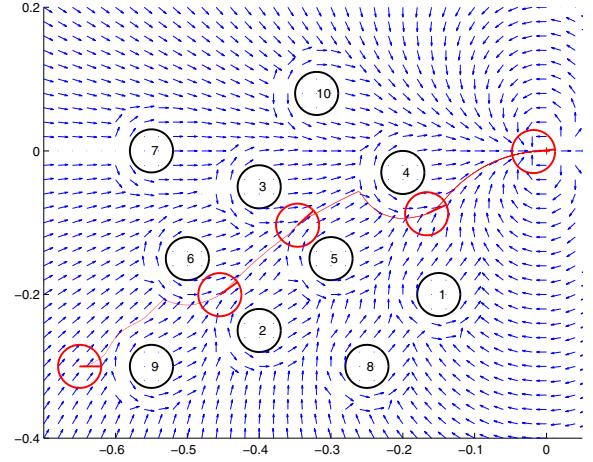


Fig. 3. Collision-free motion of a unicycle in an obstacle environment.

case as well. Let us consider the case of  $N$  circular agents  $i$  that have to move to goal configurations  $\mathbf{q}_{gi}$  while avoiding collisions among them. Clearly, each agent  $j \neq i$  serves as an obstacle to agent  $i$ . A vector field  $\mathbf{F}_i^*$  can be constructed for each agent  $i$ , where the repulsive term  $\mathbf{F}_{oj}$  around agent  $j$  is replaced with a repelling node. This is to ensure that the repelling vector field always points into the interior of the free space  $\mathcal{F}_i$  of each agent  $i$ .

In the scenario depicted in Fig. 4 four agents are moving towards their goal destinations, while avoiding collisions. Here we have assumed that there is bidirectional communication and information exchange among every pair of agents  $(i, j)$ , to argue that each agent  $i$  always knows the positions of all other agents  $j \neq i$ . Nevertheless, this assumption is *not* restrictive regarding on the proposed control design, as illustrated in [22]; the same vector field construction and control design can be used in the cases of limited sensing or given communication topologies for each agent.

#### V. CONCLUSIONS

This paper presented a novel methodology for the path and motion planning of nonholonomic (unicycle) systems in environments with obstacles, with extensions to the collision avoidance in multi-agent systems. The method is based on a family of vector fields whose integral curves exhibit either attractive or repulsive behavior, depending on the value of a parameter  $\lambda$ . It was shown that attractive-to-the-goal and repulsive-around-obstacles vector fields can be suitably blended in order to yield almost global feedback motion plans in environments with circular obstacles. The case of collision avoidance in multi-agent scenarios can be treated with the same logic as well. Thus, seeking for Lyapunov-like functions encoding the avoidance objective is not required, while no parameter tuning is needed in order to avoid local minima (stable nodes). Current work focuses on the definition of vector fields encoding input constraints, such as curvature bounds, which may be more appropriate for aircraft and car-like vehicles.



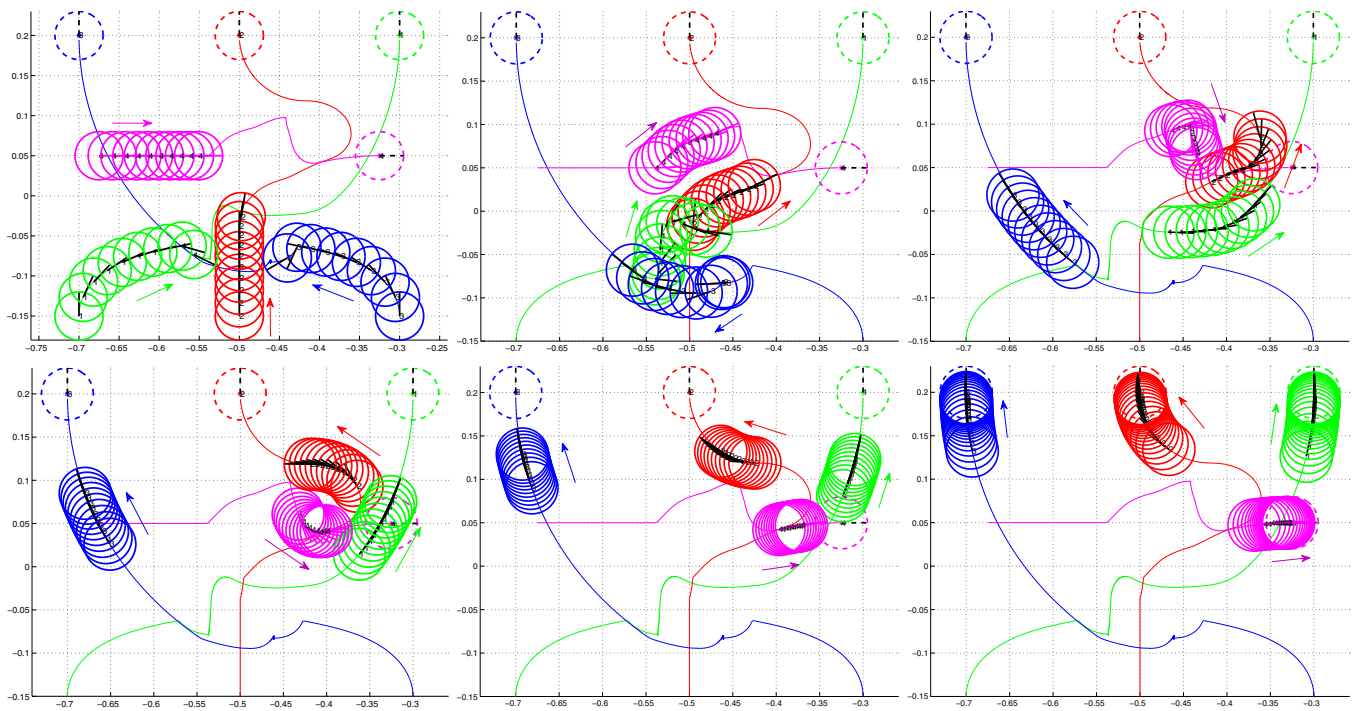


Fig. 4. Collision-free motion of 4 nonholonomic agents under the proposed control strategy.

## REFERENCES

- [1] H. Choset, K. Lynch, S. Hutchinson, G. Kantor, W. Burgard, L. Kavraki, and S. Thrun, *Principles of Robot Motion. Theory, Algorithms and Implementation*. MIT Press, 2005.
- [2] S. M. LaValle, *Planning Algorithms*. Cambridge University Press, 2006.
- [3] L. E. Parker, "Path planning and motion coordination in multiple mobile robot teams," in *Encyclopedia of Complexity and System Science*, R. A. Meyers, Ed. Springer, 2009.
- [4] W. Ren and Y. Cao, "Overview of recent research in distributed multi-agent coordination," in *Distributed Coordination of Multi-agent Networks*, ser. Communications and Control Engineering. Springer-Verlag London Limited, 2011, ch. 2, pp. 23–41.
- [5] G. Leitmann and J. Skowronski, "Avoidance control," *Journal of Optimization Theory and Applications*, vol. 23, pp. 581–591, Dec. 1977.
- [6] O. Khatib, "Real-time obstacle avoidance for manipulators and mobile robots," *The International Journal of Robotic Research*, vol. 5, no. 1, pp. 90–98, Spring, 1986.
- [7] E. G. Hernandez-Martinez and E. Aranda-Bricaire, "Convergence and collision avoidance in formation control: A survey of the artificial potential functions approach," in *Multi-Agent Systems - Modeling, Control, Programming, Simulations and Applications*, ser. Robotics. Multiagent Systems, F. Alkhateeb, E. A. Maghayreh, and I. A. Doush, Eds. InTech, 2011, ch. 6, pp. 103–126.
- [8] D. M. Stipanović, C. J. Tomlin, and G. Leitmann, "Monotone approximations of minimum and maximum functions and multi-objective problems," *Applied Mathematics and Optimization*, vol. 66, pp. 455–473, 2012.
- [9] E. Rimon and D. Koditschek, "Exact robot navigation using artificial potential functions," *IEEE Transactions on Robotics and Automation*, vol. 8, no. 5, pp. 501–518, Oct. 1992.
- [10] C. I. Connolly, J. B. Burns, and R. Weiss, "Path planning using Laplace's equation," in *Proc. of the 1990 IEEE International Conference on Robotics and Automation*, May 1990, pp. 2102–2106.
- [11] H. J. S. Feder and J.-J. E. Slotine, "Real-time path planning using harmonic potentials in dynamic environments," in *Proc. of the 1997 IEEE International Conference on Robotics and Automation*, Albuquerque, New Mexico, Apr. 1997, pp. 874–881.
- [12] P. Szulczyński, D. Pazderski, and K. Kozłowski, "Real-time obstacle avoidance using harmonic potential functions," *Journal of Automation, Mobile Robotics and Intelligent Systems*, vol. 5, no. 3, pp. 59–66, 2011.
- [13] S. Waydo and R. M. Murray, "Vehicle motion planning using stream functions," in *Proc. of the 2003 IEEE International Conference on Robotics and Automation*, Taipei, Taiwan, Sep. 2003, pp. 2484–2491.
- [14] A. D. Luca and G. Oriolo, "Local incremental planning for non-holonomic mobile robots," in *Proc. of the 1994 IEEE International Conference on Robotics and Automation*, May 1994, pp. 104–110.
- [15] S. R. Lindemann and S. M. LaValle, "Simple and efficient algorithms for computing smooth, collision-free feedback laws over given cell decompositions," *The International Journal of Robotics Research*, vol. 28, no. 5, pp. 600–621, 2009.
- [16] T. Liddy, T.-F. Lu, P. Lozo, and D. Harvey, "Obstacle avoidance using complex vector fields," in *Proc. of the 2008 Australasian Conference on Robotics and Automation*, Canberra, Australia, Dec. 2008.
- [17] J. Borenstein and Y. Koren, "Real-time obstacle avoidance for fast mobile robots," *IEEE Transactions on Systems, Man, and Cybernetics*, vol. 19, no. 5, pp. 1179–1187, Sep. 1989.
- [18] E. G. Hernández-Martínez and E. Aranda-Bricaire, "Multi-agent formation control with collision avoidance based on discontinuous vector fields," in *Proc. of the 35th Annual Conference of IEEE Industrial Electronics*, Nov. 2009, pp. 2283–2288.
- [19] D. Panagou and V. Kumar, "Maintaining visibility for leader-follower formations in obstacle environments," in *Proc. of the 2012 IEEE International Conference on Robotics and Automation*, St. Paul, Minnesota, USA, May 2012, pp. 1811–1816.
- [20] D. Panagou, H. G. Tanner, and K. J. Kyriakopoulos, "Control of nonholonomic systems using reference vector fields," in *Proc. of the 50th IEEE Conference on Decision and Control and European Control Conference*, Orlando, Florida, Dec. 2011, pp. 2831–2836.
- [21] M. Henle, *A Combinatorial Introduction to Topology*. Dover Publications, 1994.
- [22] D. Panagou, "Feedback motion planning and collision avoidance using non-gradient navigation vector fields. Technical Report." [Online]. Available: <https://uofi.box.com/shared/static/o86ri581vjwl46dpos1g.pdf>